Design of α7 nicotinic acetylcholine receptor ligands in quinuclidine, tropane and quinazoline series. Chemistry, molecular modeling, radiochemistry, in vitro and in rats evaluatio…

ARTICLE *in* EUROPEAN JOURNAL OF MEDICINAL CHEMISTRY · MAY 2014

Impact Factor: 3.45 · DOI: 10.1016/j.ejmech.2014.04.057 · Source: PubMed

13 AUTHORS, INCLUDING:

Johnny Vercouillie
University of Tours
59 PUBLICATIONS **565** CITATIONS
SEE PROFILE

Sylvie Mavel
University of Tours
59 PUBLICATIONS **570** CITATIONS
SEE PROFILE

Jean-Bernard Deloye
Laboratoires Cyclopharma
19 PUBLICATIONS **150** CITATIONS
SEE PROFILE

Sylvie Chalon
University of Tours
204 PUBLICATIONS **4,924** CITATIONS
SEE PROFILE

European Journal of Medicinal Chemistry 82 (2014) 214–224

Contents lists available at ScienceDirect

European Journal of Medicinal Chemistry

journal homepage: http://www.elsevier.com/locate/ejmech

Original article

Design of α7 nicotinic acetylcholine receptor ligands in quinuclidine, tropane and quinazoline series. Chemistry, molecular modeling, radiochemistry, *in vitro* and in rats evaluations of a [^{18}F] quinuclidine derivative

Frédéric Pin [a], Johnny Vercouillie [b], Aziz Ouach [a], Sylvie Mavel [b], Zuhal Gulhan [b], Gabrielle Chicheri [b], Christian Jarry [c], Stephane Massip [c], Jean-Bernard Deloye [d], Denis Guilloteau [b], Franck Suzenet [a], Sylvie Chalon [b, *], Sylvain Routier [a, *]

[a] Université d'Orléans, CNRS, ICOA, UMR 7311, F-45067 Orleans, France
[b] UMR Inserm U930, Université François Rabelais de Tours, CHRU de Tours, Tours, France
[c] Université de Bordeaux, Pharmacochimie, FRE CNRS 3396, 136 Rue Léo Saignat, 33076 Bordeaux Cedex, France
[d] Laboratoires Cyclopharma, Biopôle Clermont-Limagne, 63360 Saint-Beauzire, France

ARTICLE INFO

Article history:
Received 11 February 2014
Received in revised form
17 April 2014
Accepted 19 April 2014
Available online 9 May 2014

Keywords:
Alpha 7nicotinic acetylcholine receptors
Quinuclidine
Tropane
Synthesis
SAR
Radiochemistry
Molecular modeling
In vivo evaluation

ABSTRACT

In this report, we describe the synthesis of a novel library of α7 nAChR ligands based on the modulation of the quinuclidine, quinazoline and tropane moieties. Spirane derivatives were newly synthesized under stereo specific 1,3 dipolar cylcoadditions. Only amide derivatives bonded efficiently to the receptor with Ki measured between 14 and 133 nM. The best fluorinated candidate was selected and radiolabeled. The potent **[^{18}F]4** PET tracer was evaluated in rats and its brain accumulation quantified.

1. Introduction

The neurotransmitter acetylcholine (ACh) exerts its effects on the central nervous system (CNS) through two distinct muscarinic mAChRs and nicotinic nAChRs receptor types. nAChRs belong to the superfamily of ligand-gated ion channels possessing a pentameric structure [1]. These receptors are composed of multiple subunits, which have been divided into muscle-type (α1, β1, δ, γ and ε) and neuronal (α2-α10 and β2-β4) subunits [2]. In the brain, one of two major nAchRs is the α4β2 subtype, distinguished by its high affinity binding to acetylcholine and nicotine.

Homomeric α7-subtype receptors are highly permeable to calcium and are distinguished by their tight binding to α-bungarotoxin. Previous studies indicated that neuronal nicotinic receptors play important roles in modulating neurotransmission, cognition, sensory gating and anxiety [3]. Thus, there has been renewed interest in the use of nicotinic agonists to treat CNS diseases [4], such as Parkinson's disease, depression, schizophrenia, epilepsy and Alzheimer's disease (AD).

Because of their distribution and abundance in the CNS (hippocampus, cortex, cerebellum, olfactory bulb, striatum, thalamus, and spinal cord) [2], the α7 subtypes are potential therapeutic targets for these disorders. Their early reduction fully correlates with cognitive functions, favors the internalization of Aβ peptide and increases neurotoxicity. In addition, they act on signaling pathways which prevent inflammatory processes that are fully involved in AD [5]. Subsequently, α7nAChR agonists were identified

* Corresponding authors.
E-mail addresses: sylvie.chalon@univ-tours.fr (S. Chalon), sylvain.routier@univ-orleans.fr (S. Routier).

http://dx.doi.org/10.1016/j.ejmech.2014.04.057
0223-5234/

and allowed the design of novel therapeutic agents for AD. It is indubitably crucial to have in hand a human compatible [^{18}F] positron emission tomography (PET) tracer to make an early diagnosis or to validate the efficiency of drugs in clinical trials for the treatment of AD.

Several α7 receptor ligands have been reported in the literature and among them, many quinuclidine derivatives have been synthesized (Fig. 1). These aliphatic hindered tertiary amines, considered by organic chemists as a super base, have punctuated the history of medicinal chemistry and have been used as pharmacophoric elements in antibiotic structures as well as in the design of potent cannabinoid receptors, muscarinic, serotoninergic and squalene synthase inhibitors [6]. In α7 ligand discovery, this skeleton is mostly functionalized at the C-3 position by ethers [7], amides [8], carbamates [9] or ureas [10] and other representatives are also found with a C-2,-3 quinuclidinic disubstitution [11].

In addition, following a restrictive conformation strategy, several spiro derivatives have been synthesized (**I**–**II**) [12]. Lastly, the quinuclidine scaffold has been successfully engaged in a bioisosteric strategy and replaced by other polycyclic tertiary amines (**III**) in order to modulate the pharmacologic properties and explore SAR [12,13].

Based on our expertise in heterocyclic bio-mimetic development [14], we envisioned synthesizing and evaluating the potency of novel α7 nAChR ligands and their transformation into PET tracers following an approach close to one we previously used to develop a [^{18}F]-labeled tracer of the dopamine transporter. In this emerging area, only a small number of [^{11}C] short half-life tracers have been developed and even fewer [^{18}F]-labeled PET tracers have been described, such as [^{18}F]NS10743, [^{18}F]NS14490, [^{18}F]AZ11637326 and [^{18}F]**IV** (Fig 1). Most of them display low or modest brain uptake and/or a lack of specificity except [^{18}F]**IV** for which early evaluations in rodents seem promising [15]. Based on available SAR studies, we synthesized a library of potent α7 nAChR ligands containing a quinuclidine, a tropane or a 8*H*-quinolizine moiety. Some amides of type **V** were synthesized and evaluated in our biological system in order to complete unachieved SAR in those series. Original spiro isoxazoline derivatives of type **VI** and **VII** were additionally prepared using 1,3-dipolar cylcoadditions (Fig. 2).

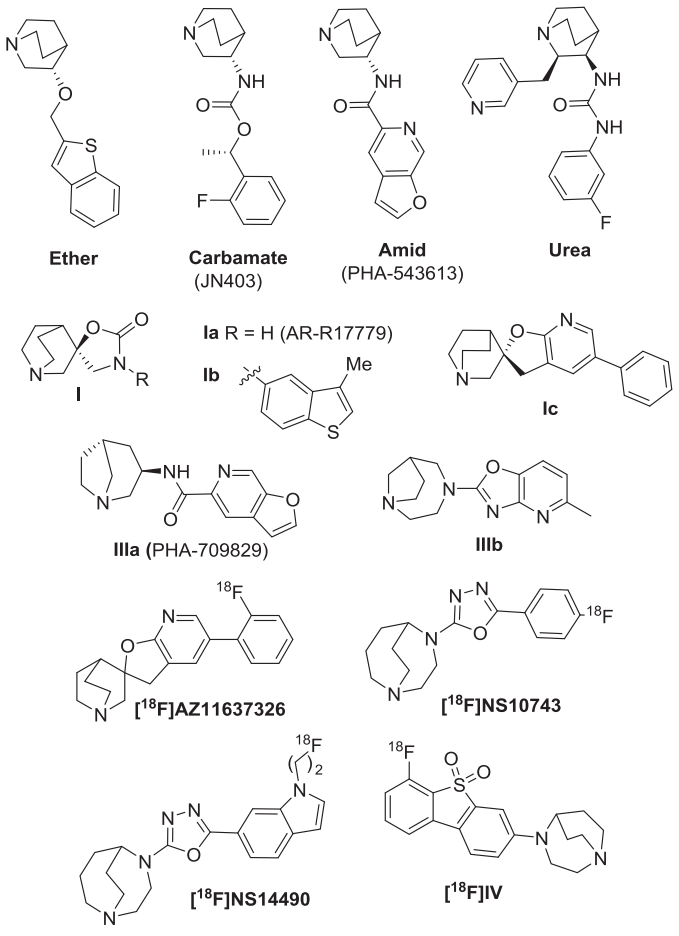

Fig. 1. Representative α7 nAchR ligands and reported ^{18}F PET imaging agents.

We report herein methods to access spirane derivatives whose structure was formally established by X-ray crystal analysis. Affinity of each final compound was determined and molecular modeling docking studies confirmed the binding mode of the best two ligands. A fluorinated derivative was selected and used to design a novel [^{18}F] α7 nAChR tracer **[^{18}F]4** which was characterized *ex vivo* in the rat. Scheme 1

2. Chemistry

2.1. Synthesis of amides V

Synthesis of amides was performed starting from quinuclidinone and tropanone derivatives to form the primary amine, stored as chlorhydrate salts **1** and **2** (Scheme 3) [16]. Freshly prepared compounds **1** and **2** were required to ensure further cycloaddition success (see section 2.2.).

Peptide bond formations were achieved from **1** and **2** using various (het)aryl carboxylic acids. Several experimental conditions were used in order to isolate the expected amides **3**–**11** in satisfactory yields. Standard molecules **3**–**6** were prepared for binding test validation according to reference procedures, while the other amides **7**–**11** were obtained using DCC and DMAP as cross coupling reagents; the use of acylchlorides in basic media gave only poor yields.

Additionally, bromo derivative **9** (Table 1, entry 7) was successfully used in a Suzuki–Miyaura reaction, using 2-thiophenyl and 2-furanyl boronic acids in a mixture of toluene/EtOH at 150 °C in presence of potassium carbonate (Scheme 2) [17]. Under microwave irradiation, cross coupling occurred very quickly and after only 20 min, final tropanamides **12** and **13** were isolated in 84% and 90% yields, respectively.

2.2. Synthesis of spiro derivatives VI and VII

The next objective was to link the tropane and the 8*H*-quinazoline scaffolds with a spiro isoxazoline skeleton. Many synthetic approaches are available to achieve the isoxazoline ring formation. Among them, we identified 1,3-dipolar cycloaddition as an interesting key step to reach the synthetic objectives in a straightforward pathway. For this purpose, the tropane or 8*H*-quinazoline exomethylenes were prepared following literature procedure and a few (het)aryl chlorooximes were prepared *in situ* just before the cycloaddition reaction.

8*H*-Quinolizin-1-one **15** was prepared following the Barker procedure [18]. A Wittig condensation starting from tropinone and **15** involving $MePPh_3Br$ in the presence of *t*-BuOK furnished exomethylene derivatives **14** [19] and **16** in good yields. The strong instability of this alkene **16** prompted us to prevent its degradation by direct preparation of its borane complex. **17** was isolated as a white solid and appeared sufficiently stable to be stored without any particular precautions.

We also freshly prepared six different (het)arylchlorooximes **24**–**29** (Table 2) *via* the condensation of the chosen aldehydes with

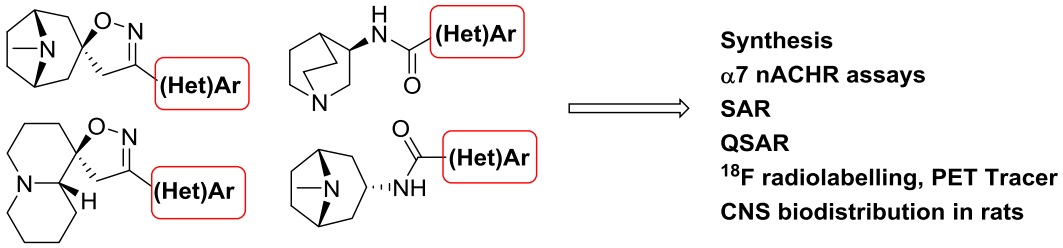

Fig. 2. Main synthetic objectives.

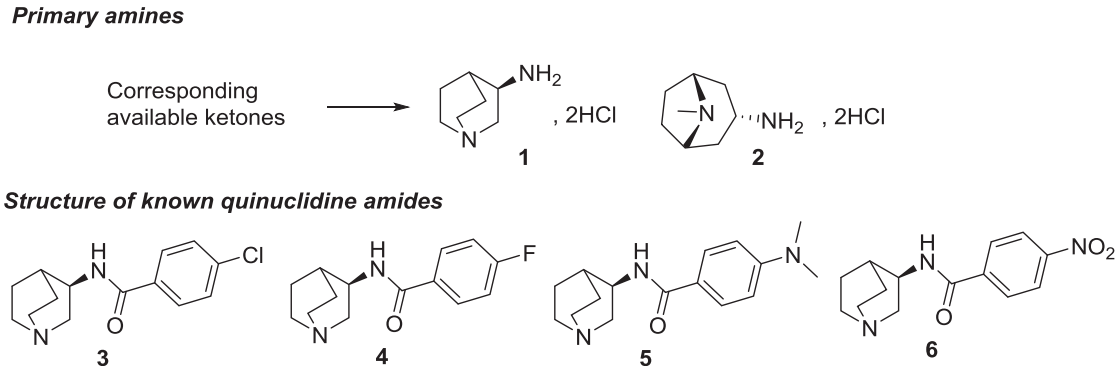

Scheme 1. Structure of useful materials **1**–**6**.

hydroxylamine hydrochloride at room temperature in presence of Et_3N (a syn/anti isomer mixture) and subsequent chlorination of the oxime intermediates **18**–**23** using NCS at 0 °C.

The exomethylene and chlorooxime reagents were engaged in a 1,3-dipolar cycloaddition [19]. A period of 24 h was necessary to complete the conversion and offer the spiro-isoxazole units. Under these optimized experimental conditions, compounds **30**–**34** were isolated in moderate yields. For each run, we were unable to prevent nitrile oxide dimerization and early degradation due to instability of chlorooximes **24**–**29**. Unfortunately, derivative **35** was not pure enough to engage it in cross coupling reactions and increase diversity. Table 3

All 1,3-dipolar cycloadditions were fully regio and stereo specific. Only one diastereoisomer of compound **30**–**34** was isolated and characterized by NMR. Isolation of a single crystal of **30** gave access to its X-ray analysis (Fig. 3). The ORTEP representation clearly shows the spiranic carbon configuration and the formation of the oxazole ring fused to the tropane moiety.

Starting from the non-basic 8*H*-quinolizine boron complex **17**, the experimental procedure was simplified. All reagents were mixed without any special precautions and spiro derivatives **36**–**41** were isolated in 49–64% yield (Table 4). BH_3 protection was removed under the reaction conditions.

Regio and stereo selectivity of the cycloaddition in quinazoline series was fully established. An X-ray analysis of **41** completed our spectroscopic data and the ORTEP representation (Fig. 4) clearly shows the quinazolin/oxazolin spiranic ligation enchainment. The *N,O* oxazolin heteroatoms direct towards the same side as the *C*-16 quinuclidine hydrogen atom. Oxazoline and bromothiophene moieties constitute a single plane.

3. *In vitro* biological assays

All synthesized compounds were evaluated for their inhibitory effect on the binding of [^{125}I]α-bungarotoxin as reference ligand. Measured affinities are reported in Table 5. In our hands, *Ki* for derivatives **3** and **4** were found in the nanomolar range whereas compounds **5** and **6** appeared less efficient at binding to α7 nAChR (Table 5, entries 1–4). These results are in agreement with the reported EC_{50} and selectivity (*vs.* 5-HT_3 receptors) for **4** and its chlorinated derivative **3** (PNU-282987), which was the most potent derivative of the series [8]. Product **4** appeared therefore as a good candidate for *in vivo* exploration of the α7 nAChR by PET after labeling with **[^{18}F]**.

More derivatives were synthesized in the tropane amide series (entries 5–11). Surprisingly, 4-chlorophenyl and thiophenyl derivatives **7** and **8** were inactive, indicating a radical change in the binding mode to receptor. Fortunately, α7 nAChR binding can be restored by increasing the size and lipophilicity of the amide substituent thanks to a bromine at the *C*-5 position of the thiophene

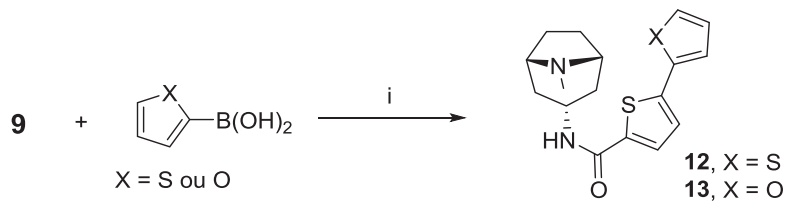

Scheme 2. *Reagents and conditions*: i) Boronic acid (1.2 eq.), $Pd(PPh_3)_4$ (10%), K_2CO_3 (2.0 eq.), toluene/EtOH (3/1) microwave irradiation, 150 °C, 20 min, **12** 84%, **13** 90%.

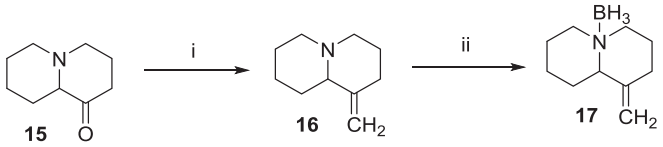

Scheme 3. *Reagents and conditions*: i) CH_3PPh_3Br (1.0 eq.), t-BuOK (1.0 eq.), THF, 0 °C, 1 h 30 then appropriate ketone (1.0 eq.), 15 h, r.t. 75%; ii) B_2H_6•THF (1.0 eq.), THF, −10 °C, 1 h, 97%.

ring. Compound **9** exhibited an encouraging *K*i of 78 nM (entry 7). Increasing the size of this aromatic substituent was detrimental for affinity. Benzofuran and benzothiophene derivatives **10** and **11** (entries 8, 9) which contain planar and aromatic fused systems showed lower affinities (a reduction of 30% was observed).

This tropane amide SAR study prompted us to introduce a bis-thiophene and a furanylthiophene substituent. Resulting derivatives **12** and **13** exhibited *K*i of 12 and 14 nM, respectively (Table 5, entries 10, 11). The latter two derivatives are indubitably lead compounds for novel SAR optimizations and for designing original ^{18}F tracers, whereas spiro derivatives of type **V** and **VI** were inactive (Ki > 1 μM).

From these *in vitro* results, a QSAR study (Discovery Studio® 2.5, Accelrys) was done to improve our knowledge of new ligands design for α7 nAChR, in order to point out molecular requirements in the tropane amide bis(het)aryl series [20–22]. The QSAR equation with the regression statistics is first given (see supplementary data, Fig. S1). As the coefficient in the equation is negative for the conformational descriptor mentioned as Apol ("Sum of atomic polarizabilities"), the less polar the structure, the higher the p*K*i. Concerning the structural properties, HBD_Count indicates the importance of "number of hydrogen bond donating groups" (one or more H-bond donating group is a plus). BIC is a "graph-theoretical info-content descriptor" concerning "Bonding Information Content". As the equation coefficient is negative, the less compact the structure is, the higher the p*K*i will be. Also as the 2D topological descriptors, IAC_Mean ("Mean Information of Atomic Composition") and IC ("Information Content", depending on the size, degree of branching and flexibility of the structure), have a positive coefficient, the higher the values, the better. The equation showed occurrences of 3D Jurs descriptors, suggesting the importance of charge distribution and surface areas (Jurs_WNSA_3 depends on total molecular solvent-accessible surface area), and should be a high value, indicative of non-compact structures.

Furthermore, a 3D-QSAR model (Discovery Studio® 2.5, Accelrys) was developed (Fig. 5). Several key features are predicted to increase α7 nAChR affinity: i) reinforcement of the negative environment in a zone 10 Å from the *N*-1 tertiary nitrogen atom (toward the second (het)aryl group); ii) decrease of the negative environment in a zone 7 Å from the *N*-1 nitrogen atom and

Table 1
Amides of type **IV** starting from **1** or **2**.

Entry	Starting material	Product (Yield)[a]	
1		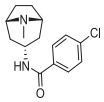	**7** (74%)
2		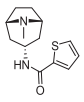	**8** (56%)
3		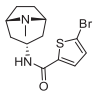	**9** (52%)
4		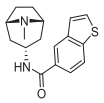	**10** (80%)
5		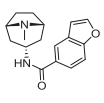	**11** (77%)

[a] Yields are indicated in isolated product. *Conditions*: Carboxylic acid (1.5 eq.), DCC (1.5 eq.), DMAP (cat.), Et_3N (3.0 eq.), CH_2Cl_2, 6 h, rflx.

Table 2
Preparation of chlorooximes **24**–**29**. *Conditions*: i) NH_2OH•HCl (1.2 eq.), Et_3N (1.5 eq.), CH_2Cl_2, r.t., 12 h; ii) NCS (1.1 eq.), DMF, 0 °C to r.t., 12 h.

Entry	Aldehyde	Oxime (yield)[a]	Chlorooxime (yield)[a]
1		**18**[b]	**24**[b]
2		**19**[b]	**25**[b]
3	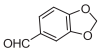	**20** (97%)[c]	**26** (71%)[c]
4	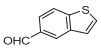	**21** (98%)[c]	**27** (84%)[c]
5	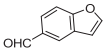	**22** (97%)[c]	**28** (68%)[c]
6		**23**[b]	**29** (94%)[c]

[a] Yields are given in isolated products.
[b] Commercially available.
[c] Synthesized compounds isolated as single products after extraction and pure enough to be used in the next step without any further purification.

Table 3
Synthesis of spiranic tropane derivatives **VI**. *Conditions*: i) chlorooxime **24**–**29** (2.0 eq.) $NaHCO_3$ (5.0 eq.), CH_2Cl_2, r.t., 72 h.

Entry	Chlorooxime	Product **VI** (Yield)[a]	
1	**24**	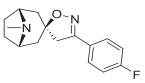	**30** (45%)
2	**25**	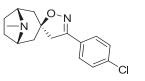	**31** (44%)
3	**26**	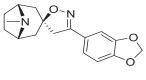	**32** (47%)
4	**27**	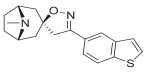	**33** (39%)
5	**28**	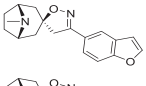	**34** (33%)
6	**29**	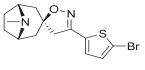	**35** (ND)

[a] Yields are indicated in isolated products. ND: Compound appears as not pure enough to be fully characterized.

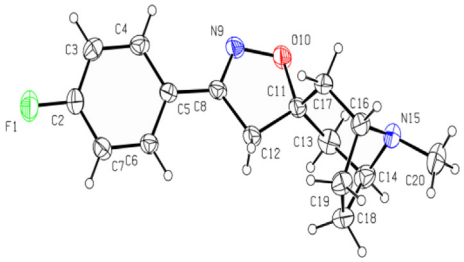

Fig. 3. ORTEP representation of X-Ray analysis of **30**.

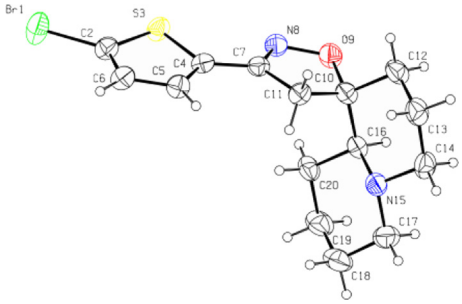

Fig. 4. ORTEP representation of X-Ray crystal structures of **41**.

minimization of the electro negativity of the first aromatic ring and iii) minimization of Van der Waals interactions around this first aromatic group. Chemical assays are also in progress to optimize our series using these preliminary 3D data.

4. Radiolabeling

Among the compounds developed, **4** demonstrated a good affinity and selectivity to α7 nAChR and presented a fluorine atom on the aromatic ring, allowing preparation of its radiofluorinated analogue.

^{18}F labeling of compound **4** was envisaged by aromatic nucleophilic substitution starting from the nitro derivative **6**. As the electron withdrawal effect of the amide function is weak, the radionuclide incorporation by conventional thermal heating was very low, around 2% (decay corrected from EOB) after 20 min reaction. We set up the reaction in a microwave designed for radionuclide applications (PET wave, CEM). Under microwave irradiation at 100 W for 10 min, yield was improved to 10% in a shorter time and afforded **[^{18}F]4** with a specific activity of 26 ± 10 GBq/μmole. Moreover, the use of microwave implies the use of an additional device compared to the thermal approach which was entirely accomplished in an FX-FN automaton (GE healthcare). It thus generates high dead volumes and considerable losses during transfer of crude product between the two devices. Scheme 4

Table 4
Synthesis of spiranic 8*H*-quinazoline derivatives **VII**. *Conditions*: i) $NaHCO_3$ (5.0 eq.), EtOAc, r.t., 72 h.

Entry	Chlorooxime	Product **VII** (Yield)[a]	
1	**24**	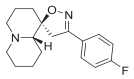	**36** (54%)
2	**25**	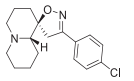	**37** (50%)
3	**26**	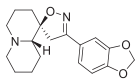	**38** (52%)
4	**27**	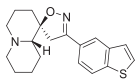	**39** (56%)
5	**28**	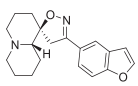	**40** (49%)
6	**29**	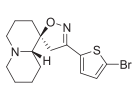	**41** (64%)

[a] Yields are indicated in isolated products.

5. *In vivo* studies

To date it can be argued that an ideal α7 nAChR tracer requires i) a passage through the blood–brain barrier followed by a preferential accumulation in brain areas known to contain α7 nAChR, ii) a decreased accumulation after the MLA α7 nAChR antagonist pretreatment as indicative for *in vivo* specific binding [23]. To evaluate these parameters, we performed preliminary brain biodistribution experiments in rats.

As can be seen in Fig. 6, **[^{18}F]4** entered the rat brain but after 1 h post i.v. injection, the residual amount of compound was low and rather homogeneously distributed between the studied regions (0.028–0.037% ID/g tissue in the control group). This result may indicate the penetration of our compound into the brain but it is possible that a very high release occurs. Although there is undoubtedly a differential blood–brain barrier crossing level depending on the animal species, it is clear that **[^{18}F]4** had a lower brain uptake in rats than the recently developed tracer **[^{18}F]IV** in mice, and that its distribution among brain regions was rather homogenous, in contrast to results obtained with **[^{18}F]IV** [15]. However, the residual amount of **[^{18}F]4** in rats pre-injected with the α7 nAChR antagonist MLA showed a slight decrease in accumulation (5–25%) in almost all studied brain regions, which could indicate a partial *in vivo* binding of our tracer to α7 nAChR. The much better affinity of **[^{18}F]IV** than **[^{18}F]4** for α7 nAChR (0.4 *vs.* 18 nM) is probably correlated with the results obtained *in vivo* and we are pursuing efforts to develop ^{18}F tropanamide and other quinuclidinic triazole series with improved affinity [24].

6. Conclusions

In this paper, we have reported the synthesis of novel amide and spiro derivatives as potent ligands for α7 nicotinic receptors. Structures of novel spiro derivatives were formally established by

Table 5
Results of *in vitro* assays.

Entry	Compound	α7 nAChR *Ki* (nM)[a,b]
1	**3**	17 ± 5 (EC_{50} = 128 nM)
2	**4**	18 ± 1 (EC_{50} = 506 nM)
3	**5**	158 ± 19 (EC_{50} = 30 μM)
4	**6**	44 ± 11 (EC_{50} = 1 μM)
5	**7**	>1 μM
6	**8**	>1 μM
7	**9**	78 ± 8
8	**10**	108 ± 2
9	**11**	133 ± 7
10	**12**	12 ± 4
11	**13**	14 ± 2

[a] Values are expressed as an average of four values ± SEM.
[b] EC_{50} values were extracted from the literature [8].

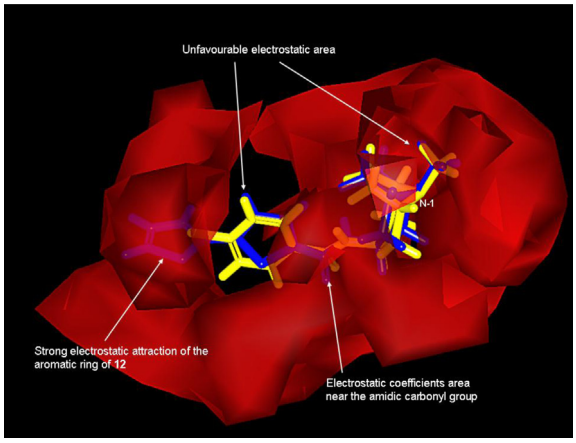

Fig. 5. Isosurface of the 3D-QSAR model coefficients on Electrostatic Potential (EP) grids with electrostatic potential in red solid representation for the aligned 22 molecular structures. Derivatives **12** (as ligand for the a-7 receptor) and **5** (as non-ligand for the a-7 receptor) are shown in blue and yellow stick representation, respectively.

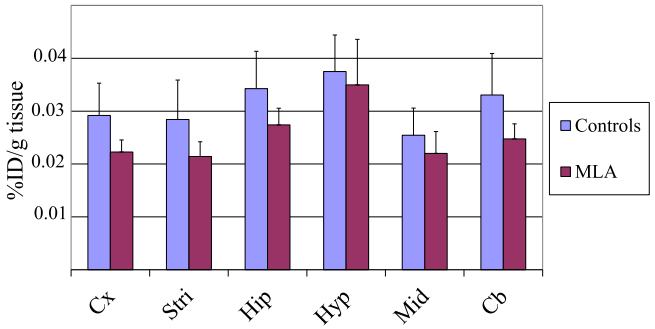

Fig. 6. Cerebral biodistribution of **[18F]4** 60 min after i.v. injection in rats. In the MLA group, animals received an i.v. pre-injection (15 min) of the α7 nicotinic receptor antagonist methyllycaconitine (3 mg/kg). Results are expressed as % injected dose/g tissue ± SD. Cx, cortex; Stri, striatum; Hip, hippocampus, Hyp, hypothalamus; Mid, midbrain, Cb, cerebellum.

X-Ray analysis. Our compound library was evaluated for its affinity to α7 nAChR. Tropane and quinuclidine amides remain the best ligands but their binding mode differs considerably. Among the quinuclidine amides, we selected the fluorinated benzamide **4** which had a rather good affinity for α7 nAChR of 18 nM. Radiolabeling of **4** led to the PET ligand **[^{18}F]4** dedicated to α7 nAChR imaging. Even if the brain biodistribution studies revealed that **[^{18}F]4** is not fully suitable as a specific *in vivo* PET tracer, this report indicates the potential of this quinuclidinic series. Other efforts are in progress in other series to increase the brain penetration and modulate the brain distribution. In tropanamide series, a novel SAR potency emerged, offering us the possibility to develop other original tracer series.

7. Experimental section

7.1. Chemistry

^{1}H NMR and ^{13}C NMR spectra were recorded on a Bruker DPX 250 MHz or 400 MHz instrument using $CDCl_3$ or DMSO-d_6. The chemical shifts are reported in parts per million (δ scale) and all coupling constant (J) values are in Hertz (Hz). The following abbreviations were used to explain the multiplicities: s (singlet), d (doublet), t (triplet), q (quartet), m (multiplet) and dd (doublet doublet). Melting points are uncorrected. IR absorption spectra were obtained on a Perkin Elmer PARAGON 1000 PC and values are reported in cm^{-1}. HRMS were recorded on a Bruker maXis mass spectrometer by the "Fédération de Recherche" ICOA/CBM (FR2708) platform. Monitoring of the reactions was performed using silica gel TLC plates (silica Merck 60 F254). Spots were visualized by UV light at 254 nm and 356 nm. Column chromatographies were performed using silica gel 60 (0.063–0.200 mm, Merck). Microwave irradiation was carried out in sealed 2–5 mL vessels placed in a Biotage Initiator system using a standard

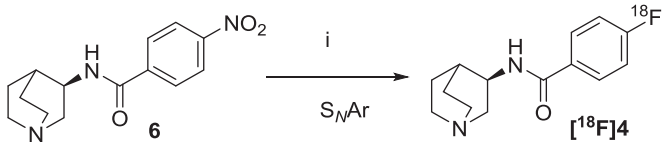

Scheme 4. *Conditions*: i) [^{18}F]KF, K_{222}, DMSO, μW irradiation 100 W, 10 min. HPLC purification and formulation.

absorbance level (300 W maximum power). The temperatures were measured externally by an IR probe that determined the temperature on the surface of the vial and could be read directly from the instrument screen. The reaction time was measured from when the reaction mixture reached the stated temperature for temperature-controlled experiments. Pressure was measured by a non-invasive sensor integrated into the cavity.

7.1.1. General procedure for the synthesis of amide derivatives 7–11

To a solution of 3-*endo*-tropanamine hydrochloride salt **2** (213 mg, 1.00 mmol) in 10 mL of CH_2Cl_2 were added successively the corresponding carboxylic acid (1.5 mmol), the *N,N′*-dicyclohexylcarbodiimide (310 mg, 1.5 mmol), the 4-dimethylaminopyridine (12.0 mg, 0.10 mmol) and the triethylamine (420 μl, 3.0 mmol). The reaction mixture was refluxed for 6 h. after cooling, the mixture was diluted with CH_2Cl_2 (10 mL) and the organic layer was washed with a saturated solution of $NaHCO_3$ (10 mL), dried over $MgSO_4$, filtered and evaporated under reduced pressure. The resulting product was purified by chromatography on a silica gel column eluting with CH_2Cl_2/MeOH/28% aq. NH_4OH (9/1/0.1) to give the expected products in appreciable yields.

7.1.2. 4-Chloro-N-[(1R,5S)-8-methyl-8-azabicyclo[3.2.1]octan-3-yl] benzamide 7

Compound **7** was prepared from the 4 chlorobenzoic acid and was isolated after purification as a white solid (205 mg, 74%). mp 170–172 °C. Rf (CH_2Cl_2/MeOH 9/1) 0.11. IR (ATR diamond, cm^{-1}) ν 760, 1016, 1046, 1088, 1141, 1291, 1340, 1486, 1519, 1593, 1630, 2922, 3351. ^{1}H NMR (250 MHz, $CDCl_3$) δ 1.70–1.90 (m, 4H), 2.20–2.25 (m, 2H), 2.30–2.40 (m, 5H), 3.26 (br s, 2H), 4.25 (q, 1H, J = 6.5 Hz), 6.49 (br s, 1H), 7.40 (d, 2H$_{Ar}$, J = 8.5 Hz), 7.66 (d, 2H$_{Ar}$, J = 8.5 Hz). ^{13}C NMR (63 MHz, $CDCl_3$) δ 26.1 (2× CH_2), 36.4 (2× CH_2), 40.3 (CH_3), 42.2 (CH), 60.3 (2× CH), 128.3 (2× CH_{Ar}), 129.2 (2× CH_{Ar}), 133.5 (C_q), 137.9 (C_q), 165.6 (C=O). HRMS (ESI): *m/z* calculated for $C_{15}H_{20}ClN_2O$ (MH^+): 279.1264; Found: 279.1259.

7.1.3. N-[(1R,5S)-8-Methyl-8-azabicyclo[3.2.1]octan-3-yl] thiophene-2-carboxamide 8

Compound **8** was prepared from the 2-thiophenecarboxylic acid and was isolated after purification as a white solid (140 mg, 56%). mp 138–140 °C. Rf (CH_2Cl_2/MeOH 9/1) 0.13. IR (ATR diamond, cm^{-1}) ν 1037, 1077, 1113, 1298, 1341, 1421, 1452, 1510, 1541, 1615, 2944, 3286. ^{1}H NMR (250 MHz, $CDCl_3$) δ 1.73–1.88 (m, 4H), 2.15–2.40 (m, 4H), 2.32 (s, 3H), 3.21 (br s, 2H), 4.25 (q, 1H, J = 6.7 Hz), 6.35 (br s, 1H), 7.08 (dd, 1H$_{Ar}$, J = 3.9 Hz, 0.9 Hz), 7.44–7.48 (m, 2H$_{Ar}$). ^{13}C NMR (63 MHz, $CDCl_3$) δ 26.1 (2× CH_2), 36.5

(2× CH_2), 40.3 (CH_3), 42.1 (CH), 60.2 (2× CH), 127.9 (CH_{Ar}), 128.1 (CH_{Ar}), 129.8 (CH_{Ar}), 139.5 (C_q), 161.1 (C═O). HRMS (ESI): *m/z* calculated for $C_{13}H_{19}N_2OS$ (MH^+): 251.1218; Found: 251.1213.

7.1.4. 5-Bromo-N-[(1R,5S)-8-methyl-8-azabicyclo[3.2.1]octan-3-yl] thiophene-2-carboxamide 9

Compound **9** was prepared from the 5-bromothiophene-2-carboxylic acid and was isolated after purification as a white solid (170 mg, 52%). mp 197–199 °C. R_f (CH_2Cl_2/MeOH 9/1) 0.18. IR (ATR diamond, cm^{-1}) ν 747, 1039, 1104, 1290, 1420, 1435, 1540, 1622, 2905, 3326. ^1H NMR (250 MHz, $CDCl_3$) δ 1.65–1.8 (m, 4H), 2.10–2.30 (m, 4H), 2.31 (s, 3H), 3.20 (br s, 2H), 4.21 (q, 1H, J = 6.9 Hz), 6.19 (br s, 1H), 7.04 (d, $1H_{Ar}$, J = 3.9 Hz), 7.18 (d, $1H_{Ar}$, J = 3.9 Hz). ^{13}C NMR (63 MHz, $CDCl_3$) δ 26.1 (2× CH_2), 36.4 (2× CH_2), 40.3 (CH_3), 42.2 (CH), 60.2 (2× CH), 117.7 (C_q), 128.0 (CH_{Ar}), 130.9 (CH_{Ar}), 140.8 (C_q), 160.0 (C═O). HRMS (ESI): *m/z* calculated for $C_{13}H_{18}BrN_2OS$ (MH^+): 329.0323; Found: 329.0335.

7.1.5. N-[(1R,5S)-8-Methyl-8-azabicyclo[3.2.1]octan-3-yl] benzothio- phene-5-carboxamide 10

Compound **10** was prepared from the 1-benzothiophene-5-carboxylic acid and was isolated after purification as a white solid (240 mg, 80%). mp 154–156 °C. R_f (CH_2Cl_2/MeOH 9/1) 0.15. IR (ATR diamond, cm^{-1}) ν 757, 1044, 1102, 1147, 1253, 1339, 1436, 1532, 1625, 2911, 3309. ^1H NMR (400 MHz, $CDCl_3$) δ 1.79 (d, 2H, J = 14.4 Hz), 1.84–1.95 (m, 2H), 2.18–2.25 (m, 2H), 2.28–2.35 (m, 5H), 3.21 (br s, 2H), 4.30 (q, 1H, J = 6.8 Hz), 6.56 (d, 1H, J = 6.3 Hz), 7.40 (d, $1H_{Ar}$, J = 5.4 Hz), 7.52 (d, $1H_{Ar}$, J = 5.4 Hz), 7.67 (dd, $1H_{Ar}$, J = 8.4 Hz, J = 1.6 Hz), 7.92 (d, $1H_{Ar}$, J = 8.4 Hz), 8.20 (d, $1H_{Ar}$, J = 1.6 Hz). ^{13}C NMR (100 MHz, $CDCl_3$) δ 26.2 (2× CH_2), 36.6 (2× CH_2), 40.4 (CH_3), 42.2 (CH), 60.2 (2× CH), 122.3 (CH_{Ar}), 122.5 (CH_{Ar}), 122.9 (CH_{Ar}), 124.4 (CH_{Ar}), 128.2 (CH_{Ar}), 131.6 (C_q), 139.7 (C_q), 142.8 (C_q), 166.8 (C═O). HRMS (ESI): *m/z* calculated for $C_{17}H_{21}N_2OS$ (MH^+): 301.1375; Found: 301.1373.

7.1.6. N-[(1R,5S)-8-Methyl-8-azabicyclo[3.2.1]octan-3-yl]benzo furan-5-carboxamide 11

Compound **11** was prepared from the 1-benzofuran-5-carboxylic acid and was isolated after purification as a white solid (218 mg, 77%). mp 135–137 °C. R_f (CH_2Cl_2/MeOH 9/1) 0.16. IR (ATR diamond, cm^{-1}) ν 731, 1025, 1110, 1130, 1299, 1345, 1434, 1459, 1536, 1631, 2933, 3319. ^1H NMR (400 MHz, $CDCl_3$) δ 1.80 (d, 2H, J = 14.6 Hz), 1.86–1.92 (m, 2H), 2.14–2.26 (m, 2H), 2.30–2.40 (m, 5H), 3.24 (br s, 2H), 4.30 (q, 1H, J = 6.8 Hz), 6.50 (d, 1H, J = 5.9 Hz), 6.84 (d, $1H_{Ar}$, J = 2.0 Hz), 7.54 (d, $1H_{Ar}$, J = 8.6 Hz), 7.63–7.71 (m, $2H_{Ar}$), 8.00 (d, $1H_{Ar}$, J = 1.6 Hz). ^{13}C NMR (100 MHz, $CDCl_3$) δ 26.2 (2× CH_2), 36.4 (2× CH_2), 40.3 (CH_3), 42.1 (CH), 60.3 (2× CH), 107.2 (CH_{Ar}), 111.7 (CH_{Ar}), 120.5 (CH_{Ar}), 123.2 (CH_{Ar}), 127.9 (C_q), 130.4 (C_q), 146.6 (CH_{Ar}), 156.7 (C_q), 166.9 (C═O). HRMS (ESI): *m/z* calculated for $C_{17}H_{21}N_2O_2$ (MH^+): 285.1603; Found: 285.1606.

7.1.7. N-[(1R,5S)-8-Methyl-8-azabicyclo[3.2.1]octan-3-yl]-5-(2-thienyl)thiophene-2-carboxamide 12

Under argon, in a sealed vial, compound **9** (100 mg, 0.30 mmol) was dissolved in a mixture of toluene/EtOH (3/1, 4 mL), and 2-thiophene boronic acid (47 mg, 0.36 mmol), K_2CO_3 (85 mg, 0.60 mmol) and $Pd(PPh_3)_4$ (18 mg, 15.6 μmol) were successively added. The reaction mixture was heated under microwave irradiation at 150 °C for 15 min. After cooling, water (15 mL) was added, and extractions were performed with CH_2Cl_2 (2× 15 mL). The combined organic layers were dried with $MgSO_4$, filtered and the volatiles were removed under reduced pressure. The crude residue was purified by flash chromatography using silica gel eluting with CH_2Cl_2/MeOH/NH_4OH (9/1/0.1) to afford compound **12** (85 mg, 84%) as a white solid. mp > 250 °C. R_f (CH_2Cl_2/MeOH 9/1) 0.15. IR (ATR diamond, cm^{-1}) ν 714, 1036, 1076, 1116, 1291, 1339, 1434, 1452, 1526, 1611, 1629, 2931, 3317. ^1H NMR (400 MHz, DMSO-d_6) δ 1.82–2.24 (m, 8H), 2.32 (s, 3H), 3.27 (br s, 2H), 3.92 (q, 1H, J = 6.9 Hz), 7.15 (dd, $1H_{Ar}$, J = 3.5 Hz, J = 5.0 Hz), 7.36 (d, $1H_{Ar}$, J = 3.9 Hz), 7.45 (d, $1H_{Ar}$, J = 3.5 Hz), 7.62 (d, $1H_{Ar}$, J = 5.0 Hz), 7.77 (d, $1H_{Ar}$, J = 3.9 Hz), 8.04 (d, 1H, J = 3.6 Hz). ^{13}C NMR (100 MHz, DMSO-d_6) δ 24.8 (2× CH_2), 34.2 (2× CH_2), 39.2 (CH_3), 41.5 (CH), 59.6 (2× CH), 124.2 (CH_{Ar}), 125.1 (CH_{Ar}), 126.5 (CH_{Ar}), 128.5 (CH_{Ar}), 129.4 (CH_{Ar}), 135.8 (C_q), 138.3 (C_q), 140.4 (C_q), 160.9 (C═O). HRMS (ESI): *m/z* calculated for $C_{17}H_{21}N_2OS_2$ (MH^+): 333.1095; Found: 333.1091.

7.1.8. 5-(2-Furyl)-N-[(1R,5S)-8-methyl-8-azabicyclo[3.2.1] octan-3-yl] thiophene-2-carboxamide 13

Compound **13** was synthesized as described for **12**, starting from furan-2-boronic acid (41 mg, 0.36 mmol), and was purified by flash chromatography using silica gel eluting with CH_2Cl_2/MeOH/NH_4OH (9/1/0.1) as a white solid (85 mg, 90%). mp > 250 °C. R_f (CH_2Cl_2/MeOH 9/1) 0.16. IR (ATR diamond, cm^{-1}) ν 747, 1013, 1086, 1112, 1289, 1341, 1439, 1514, 1536, 1616, 1630, 2925, 3326. ^1H NMR (400 MHz, DMSO-d_6) δ 1.89–2.30 (m, 8H), 2.38 (s, 3H), 3.37 (br s, 2H), 3.93 (q, 1H, J = 6.9 Hz), 6.66 (dd, 1H, J = 3.4 Hz, J = 1.8 Hz), 6.94 (d, $1H_{Ar}$, J = 3.4 Hz), 7.41 (d, $1H_{Ar}$, J = 3.9 Hz), 7.77–7.87 (m, $2H_{Ar}$), 8.11 (d, 1H, J = 3.6 Hz). ^{13}C NMR (100 MHz, DMSO-d_6) δ 24.5 (2× CH_2), 33.7 (2× CH_2), 39.1 (CH_3), 41.3 (CH), 59.9 (2× CH), 107.2 (CH_{Ar}), 112.4 (CH_{Ar}), 123.0 (CH_{Ar}), 129.3 (CH_{Ar}), 136.5 (C_q), 138.1 (C_q), 143.3 (CH_{Ar}), 148.0 (C_q), 161.1 (C═O). HRMS (ESI): *m/z* calculated for $C_{17}H_{21}N_2O_2S$ (MH^+): 317.1324; Found: 317.1312.

7.1.9. Borane-9-methylene-8H-quinolizine complex 17

Under argon at −10 °C, a solution of B_2H_6•THF (1 M in THF) (9.0 mL, 9.0 mmol) was added dropwise to a solution of the olefin **16** (1.36 g, 9.0 mmol) in 75 mL of dry THF. The mixture was stirred at the same temperature for 1 h. A brine solution (30 mL) was added and the layers were separated. The aqueous layer was extracted with ethyl acetate (2 × 50 mL) and the organic layers were combined, dried over $MgSO_4$ and evaporated under reduced pressure. The resulting white precipitate was filtered and washed with petroleum ether (20 mL) to give the borane tertiary derivative **17** (1.44 g, 97%) as a white solid. R_f (petroleum ether/EtOAc 9/1) 0.89. mp 97–99 °C. IR (ATR diamond, cm^{-1}) ν 916, 1033, 1137, 1295, 1397, 3277. ^1H NMR (250 MHz, $CDCl_3$) δ 1.25–1.73 (m, 7H), 1.85–2.02 (m, 1H), 2.07–2.29 (m, 2H), 2.39–2.66 (m, 5H), 2.82 (d, 1H, J = 11.8 Hz), 3.14 (d, 2H, J = 9.5 Hz), 4.81 (s, 1H), 4.97 (s, 1H). ^{13}C NMR (63 MHz, $CDCl_3$) δ 21.1 (CH_2), 21.8 (CH_2), 23.6 (CH_2), 24.4 (CH_2), 33.9 (CH_2), 65.0 (CH_2), 65.8 (CH_2), 69.6 (CH), 111.4 (CH_2), 142.9 (C_q). MS (ESI): *m/z* 152.5 ($M + H^+$).

7.1.10. General procedure for the synthesis of oximes 18–23

The chosen aldehyde (5.0 mmol) was dissolved in dry CH_2Cl_2 (10 mL). Then, triethylamine (1.05 mL, 7.5 mmol) and hydroxylamine hydrochloride (420 mg, 6.0 mmol) were added to the above solution and the mixture was stirred for 12 at room temperature. The reaction was diluted with CH_2Cl_2 (10 mL), washed with a saturated solution of $NaHCO_3$ (10 mL), dried over $MgSO_4$ and evaporated under reduced pressure. Oximes were obtained as a mixture of syn and anti stereoisomers. A simple chromatography on a silica gel led to enough pure compound (verified by ^1H NMR) to convert them into chlorooxime derivative.

7.1.11. General procedure for the synthesis of chlorooximes 24–29

At 0 °C, the *syn* and *anti* oxime **18**–**23** (7.0 mmol) was dissolved in dry DMF (30 mL) and the *N*-chlorosuccinimide (1.03 g, 7.7 mmol) was slowly added. The reaction was stirred for 12 h and the solvent was carefully evaporated under reduced pressure (without heating above 40 °C). The residue was solubilized into ethyl acetate (30 mL)

and washed five times with water (50 mL). The organic layer was dried over anhydrous $MgSO_4$ and carefully concentrated under vacuum to afford the crude chlorooxime **24**–**29**. Their purities were verified by ^1H NMR prior to use the chlorooximes in the next cycloaddition step.

7.1.12. General procedure A for the synthesis of spiranic derivatives 30, 31, 32 and 34

A solution of chlorooximes **24**–**28** (2.0 mmol) in CH_2Cl_2 (10 mL) in a gas-tight syringe was added *via* a syringe pump over 48 h to a solution of exomethylene (**14**) (137 mg, 1.0 mmol) and $NaHCO_3$ (420 mg, 5.0 mmol) in dry CH_2Cl_2 (20 mL). The reaction was then stirred at ambient temperature for a further 24 h period which was achieved by addition of water (15 mL). The layers were separated, and the aqueous phase was extracted with CH_2Cl_2 (2 × 10 mL). The organic extracts were combined and washed with brine (10 mL), dried over anhydrous sodium sulfate, filtered and concentrated under reduced pressure. A flash column chromatography on silica gel, eluting with CH_2Cl_2/MeOH/NH_4OH (9/1/0.1) afforded the title compound **30**–**34**.

7.1.13. (1′R,5′S)-3-(4-fluorophenyl)-8′-methyl-spiro[4H-isoxazole-5,3′-8-azabicyclo[3.2.1]octane] 30

Compound **30** was obtained as described in general procedure **A** from chlorooxime **24** as a white solid (123 mg, 45%). mp 122–124 °C. R_f (CH_2Cl_2/MeOH 9/1) 0.22. IR (ATR diamond, cm^{-1}) ν 837, 917, 1067, 1089, 1159, 1219, 1351, 1412, 1427, 1513, 1605, 1933. ^1H NMR (400 MHz, $CDCl_3$) δ 1.73–1.84 (m, 4H), 2.03–2.10 (m, 2H), 2.32 (dd, 2H, J = 13.8 Hz, 3.1 Hz), 2.39 (s, 3H), 3.29 (s, 2H), 3.31 (s, 2H), 7.07 (t, $2H_{Ar}$, J = 8.6 Hz), 7.62 (dd, $2H_{Ar}$, J = 8.6 Hz, J = 3.2 Hz).^{13}C NMR (100 MHz, $CDCl_3$) δ 26.1 (2× CH_2), 38.2 (CH_3), 40.6 (2× CH_2), 48.8 (CH_2), 60.3 (2× CH), 85.1 (C_q), 116.0 (d, 2× CH_{Ar}, J = 21.9 Hz), 126.6 (d, C_q, J = 3.4 Hz), 128.5 (d, 2× CH_{Ar}, J = 8.3 Hz), 155.2 (C_q), 169.8 (d, C_q, J = 250.3 Hz). HRMS (ESI): *m/z* calculated for $C_{16}H_{20}FN_2O$ (MH^+): 275.1560; Found: 275.1566.

7.1.14. (1′R,5′S)-3-(4-chlorophenyl)-8′-methyl-spiro[4H-isoxazole-5,3′-8-azabicyclo[3.2.1]octane] 31

Compound **31** was obtained as described in general procedure **A** from chlorooxime **25** as a white solid (127 mg, 44%). mp 155–157 °C. R_f (CH_2Cl_2/MeOH 9/1) 0.30. IR (ATR diamond, cm^{-1}) ν 914, 975, 1011, 1068, 1087, 1135, 1216, 1231, 1346, 1402, 1425, 1452, 1491, 1552, 1593, 2937, 2962. ^1H NMR (400 MHz, $CDCl_3$) δ 1.74–1.84 (m, 4H), 2.05–2.12 (m, 2H), 2.32 (dd, 2H, J = 13.9 Hz, J = 3.3 Hz), 2.40 (s, 3H), 3.31 (br s, 4H), 7.35 (d, $2H_{Ar}$, J = 8.6 Hz), 7.58 (d, $2H_{Ar}$, J = 8.6 Hz). ^{13}C NMR (100 MHz, $CDCl_3$) δ 26.1 (2× CH_2), 38.1 (CH_3), 40.6 (2× CH_2), 48.6 (CH_2), 60.2 (2× CH), 85.3 (C_q), 127.8 (2× CH_{Ar}), 128.9 (C_q), 129.1 (2× CH_{Ar}), 135.9 (C_q), 155.3 (C_q). HRMS (ESI): *m/z* calculated for $C_{16}H_{20}ClN_2O$ (MH^+): 291.1264; Found: 291.1249.

7.1.15. (1′R,5′S)-3-(1,3-benzodioxol-5-yl)-8′-methyl-spiro[4H-isoxa-zole-5,3′-8-azabicyclo[3.2.1]octane] 32

Compound **32** was obtained as described in general procedure **A** from chlorooxime **26** as a white solid (141 mg, 47%). mp > 250 °C. R_f (CH_2Cl_2/MeOH 9/1) 0.14. IR (ATR diamond, cm^{-1}) ν 918, 976, 1031, 1101, 1236, 1259, 1379, 1434, 1453, 1504, 2502. ^1H NMR (400 MHz, $CDCl_3$) δ 1.70–1.82 (m, 4H), 2.00–2.20 (m, 2H), 2.32 (dd, 2H, J = 14.1 Hz, J = 3.3 Hz), 2.42 (s, 3H), 3.29 (s, 2H), 3.32 (br s, 2H), 6.00 (s, 2H), 6.81 (d, $1H_{Ar}$, J = 8.1 Hz), 7.00 (dd, $1H_{Ar}$, J = 8.1 Hz, J = 1.5 Hz), 7.26 (d, $1H_{Ar}$, J = 1.5 Hz). ^{13}C NMR (100 MHz, $CDCl_3$) δ 26.1 (2× CH_2), 37.9 (CH_3), 40.4 (2× CH_2), 49.0 (CH_2), 60.3 (2× CH), 84.5 (C_q), 101.6 (CH_2), 106.5 (CH_{Ar}), 108.3 (CH_{Ar}), 121.2 (CH_{Ar}), 124.5 (C_q), 148.3 (C_q), 149.3 (C_q), 155.8 (C_q). HRMS (ESI): *m/z* calculated for $C_{17}H_{21}N_2O_3$ (MH^+): 301.1552; Found: 301.1537.

7.1.16. (1′R,5′S)-3-(benzothiophen-5-yl)-8′-methyl-spiro[4H-isoxazole-5,3′-8-azabicyclo[3.2.1]octane] 33

Compound **33** was obtained as described in general procedure **A** from chlorooxime **27** as a white solid (121 mg, 39%). mp 162–164 °C. R_f (CH_2Cl_2/MeOH 9/1) 0.31. IR (ATR diamond, cm^{-1}) ν 931, 1049, 1105, 1148, 1236, 1309, 1363, 2923. ^1H NMR (400 MHz, $CDCl_3$) δ 1.79–1.97 (m, 4H), 2.08–2.27 (m, 2H), 2.40 (dd, 2H, J = 14.1 Hz, J = 3.0 Hz), 2.49 (s, 3H), 3.40 (br s, 2H), 3.44 (s, 2H), 7.36 (d, $1H_{Ar}$, J = 5.4 Hz), 7.49 (d, $1H_{Ar}$, J = 5.4 Hz), 7.76 (d, $1H_{Ar}$, J = 8.5 Hz), 7.88 (d, $1H_{Ar}$, J = 8.5 Hz), 7.97 (s, $1H_{Ar}$). ^{13}C NMR (100 MHz, $CDCl_3$) δ 26.0 (2× CH_2), 37.7 (CH_3), 40.2 (2× CH_2), 48.9 (CH_2), 60.4 (2× CH), 84.4 (C_q), 122.0 (CH_{Ar}), 122.4 (CH_{Ar}), 123.0 (CH_{Ar}), 124.2 (CH_{Ar}), 126.6 (C_q), 127.8 (CH_{Ar}), 139.8 (C_q), 141.3 (C_q), 156.4 (C_q). HRMS (ESI): *m/z* calculated for $C_{18}H_{21}N_2OS$ (MH^+): 313.1375; Found: 313.1375.

7.1.17. (1′R,5′S)-3-(benzofuran-5-yl)-8′-methyl-spiro[4H-isoxazole-5,3′-8-azabicyclo[3.2.1]octane] 34

Compound **34** was obtained as described in general procedure **A** from chlorooxime **28** as a yellow solid (98 mg, 33%). mp > 250 °C. R_f (CH_2Cl_2/MeOH 9/1) 0.17. IR (ATR diamond, cm^{-1}) ν 929, 1026, 1106, 1131, 1173, 1231, 1264, 1346, 1367, 1437, 1477, 1615, 2550, 3405.^1H NMR (400 MHz, DMSO-d_6) δ 2.05–2.22 (m, 6H), 2.33 (d, 2H, J = 12.7 Hz), 2.58 (s, 3H), 3.31 (br s, 2H), 3.65 (s, 2H), 7.06 (d, $1H_{Ar}$, J = 2.1 Hz), 7.68–7.76 (m, $2H_{Ar}$), 8.01 (s, $1H_{Ar}$), 8.10 (d, $1H_{Ar}$, J = 2.1 Hz). ^{13}C NMR (100 MHz, DMSO-d_6) δ 23.4 (2× CH_2), 39.6 (CH_3), 39.8 (2× CH_2), 47.2 (CH_2), 61.4 (2× CH), 82.5 (C_q), 106.9 (CH_{Ar}), 111.6 (CH_{Ar}), 120.2 (CH_{Ar}), 122.8 (CH_{Ar}), 124.8 (C_q), 127.4 (C_q), 147.1 (CH_{Ar}), 154.9 (C_q), 156.7 (C_q). HRMS (ESI): *m/z* calculated for $C_{18}H_{21}N_2O_2$ (MH^+): 297.1603; Found: 297.1606.

7.1.18. General procedure B for the synthesis of spiranic derivatives 36–41

To a suspension of borane-9-methylene-8*H*-quinolizine complex (200 mg, 1.21 mmol) and potassium carbonate (508 mg, 6.05 mmol) in ethyl acetate (15 mL) were added the corresponding chlorooximes (2.42 mmol). The reaction mixture was stirred at room temperature for 48 h. after completion of the cycloaddition, the solvent was evaporated and the residue was purified by silica gel column chromatography eluting with CH_2Cl_2/MeOH/NH_4OH (9/1/0.1) to afford the corresponding spiranic adduct.

7.1.19. (9S,9aS)-3′-(4-fluorophenyl)-spiro[8H-quinolizine-9,5′-4H-isoxazole] 36

Compound **36** was obtained as described in general procedure **B** from chlorooxime **24** as a white solid (188 mg, 54%). mp 102–104 °C. R_f 0.15. IR (ATR diamond, cm^{-1}) ν 915, 1103, 1118, 1130, 1166, 1221, 1290, 1355, 1443, 1514, 1603, 2940. ^1H NMR (400 MHz, $CDCl_3$): δ 0.89–1.06 (m, 1H), 1.14–1.31 (m, 1H), 1.40–1.87 (m, 7H), 1.90–2.12 (m, 4H), 2.75–2.96 (m, 3H), 3.48 (d, 1H, J = 17.2 Hz), 7.02–7.13 (m, $2H_{Ar}$), 7.61–7.70 (m, $2H_{Ar}$). ^{13}C NMR (100 MHz, $CDCl_3$): δ 23.1 (CH_2), 24.0 (CH_2), 24.8 (CH_2), 25.9 (CH_2), 37.2 (CH_2), 40.6 (CH_2), 56.5 (CH_2), 56.9 (CH_2), 68.2 (CH), 88.2 (C_q), 116.0 (d, 2× CH_{Ar}, J = 21.9 Hz), 126.3 (d, C_q, J = 3.3 Hz), 128.6 (d, 2× CH_{Ar}, J = 8.4 Hz), 155.3 (C_q), 163.8 (d, C_q, J = 250.3 Hz). HRMS (ESI): *m/z* calculated for $C_{17}H_{22}FN_2O$ (MH^+): 289.1716; Found: 289.1707.

7.1.20. (9S,9aS)-3′-(4-chlorophenyl)-spiro[8H-quinolizine-9,5′-4H-isoxazole] 37

Compound **37** was obtained as described in general procedure **B** from chlorooxime **25** as a white solid (184 mg, 50%). mp 133–135 °C. R_f (CH_2Cl_2/MeOH 9/1) 0.19. IR (ATR diamond, cm^{-1}) ν 1014, 1027, 1090, 1107, 1119, 1289, 1352, 1405, 1442, 1495, 1596, 2934. ^1H NMR (400 MHz, $CDCl_3$) δ 0.91–1.02 (m, 1H), 1.19–1.30 (m, 1H), 1.48 (q, 1H, J = 12.8 Hz), 1.55–1.80 (m, 6H), 1.92–2.10 (m, 4H),

2.75–2.94 (m, 2H), 2.92 (d, 1H, J = 17.2 Hz), 3.47 (s, 1H, J = 17.2 Hz), 7.37 (d, 2H$_{Ar}$, J = 8.5 Hz), 7.60 (d, 2H$_{Ar}$, J = 8.5 Hz). ^{13}C NMR (100 MHz, $CDCl_3$) δ 23.1 (CH_2), 24.0 (CH_2), 24.8 (CH_2), 25.8 (CH_2), 37.2 (CH_2), 40.4 (CH_2), 56.5 (CH_2), 56.8 (CH_2), 68.2 (CH), 88.5 (C_q), 127.9 (2× CH_{Ar}), 128.6 (C_q), 129.2 (2× CH_{Ar}), 136.0 (C_q), 155.4 (C_q). HRMS (ESI): *m/z* calculated for $C_{17}H_{22}ClN_2O$ (MH^+): 305.1421; Found: 305.1432.

7.1.21. (9S,9aS)-3′-(1,3-benzodioxol-5-yl)-spiro[8H-quinolizine-9,5′-4H-isoxazole] 38

Compound **38** was obtained as described in general procedure **B** from chlorooxime **26** as a white solid (198 mg, 52%). mp 218–220 °C. R_f (CH_2Cl_2/MeOH 9/1) 0.25. IR (ATR diamond, cm^{-1}) ν 920, 1035, 1114, 1222, 1250, 1348, 1453, 1496, 2930. ^{1}H NMR (400 MHz, $CDCl_3$) δ 0.85–1.05 (m, 1H), 1.12–1.31 (m, 1H), 1.39–1.83 (m, 7H), 1.87–2.10 (m, 4H), 2.75–2.89 (m, 3H), 3.44 (d, 1H, J = 17.2 Hz), 5.97 (s, 2H), 6.79 (d, 1H$_{Ar}$, J = 8.1 Hz), 7.02 (dd, 1H$_{Ar}$, J = 8.1 Hz, J = 1.7 Hz), 7.26 (d, 1H$_{Ar}$, J = 1.7 Hz). ^{13}C NMR (100 MHz, $CDCl_3$) δ 23.1 (CH_2), 24.0 (CH_2), 24.7 (CH_2), 25.8 (CH_2), 37.2 (CH_2), 40.7 (CH_2), 56.5 (CH_2), 56.8 (CH_2), 68.3 (CH), 87.8 (C_q), 101.6 (CH_2), 106.5 (CH_{Ar}), 108.3 (CH_{Ar}), 121.4 (CH_{Ar}), 124.2 (C_q), 148.2 (C_q), 149.3 (C_q), 155.8 (C_q). HRMS (ESI): *m/z* calculated for $C_{18}H_{23}N_2O_3$ (MH^+): 315.1709; Found: 315.1693.

7.1.22. (9S,9aS)-3′-(benzothiophen-5-yl)-spiro[8H-quinolizine-9,5′-4H-isoxazole] 39

Compound **39** was obtained as described in general procedure **B** from chlorooxime **27** as a white solid (220 mg, 56%). mp 113–115 °C. R_f (CH_2Cl_2/MeOH 9/1) 0.22. IR (ATR diamond, cm^{-1}) ν 933, 1025, 1055, 1119, 1183, 1288, 1366, 1442, 2749, 2795, 2866, 2934. ^{1}H NMR (400 MHz, $CDCl_3$) δ 0.95–1.10 (m, 1H), 1.14–1.34 (m, 1H), 1.38–1.88 (m, 7H), 1.93–2.15 (m, 4H), 2.76–2.98 (m, 2H), 3.04 (d, 1H, J = 17.2 Hz), 3.60 (d, 1H, J = 17.2 Hz), 7.35 (d, 1H$_{Ar}$, J = 5.4 Hz), 7.49 (d, 1H$_{Ar}$, J = 5.4 Hz), 7.77 (dd, 1H$_{Ar}$, J = 8.5 Hz, 1.4 Hz), 7.88 (d, 1H$_{Ar}$, J = 8.5 Hz), 8.01 (d, 1H$_{Ar}$, J = 1.4 Hz). ^{13}C NMR (100 MHz, $CDCl_3$) δ 23.2 (CH_2), 24.1 (CH_2), 24.8 (CH_2), 25.9 (CH_2), 37.2 (CH_2), 40.8 (CH_2), 56.6 (CH_2), 56.9 (CH_2), 68.4 (CH), 88.0 (C_q), 122.2 (CH_{Ar}), 122.4 (CH_{Ar}), 123.0 (CH_{Ar}), 124.3 (CH_{Ar}), 126.4 (C_q), 127.7 (CH_{Ar}), 139.8 (C_q), 141.2 (C_q), 156.5 (C_q). HRMS (ESI): *m/z* calculated for $C_{19}H_{23}N_2OS$ (MH^+): 327.1531; Found: 327.1534.

7.1.23. (9S,9aS)-3′-(benzofuran-5-yl)-spiro[8H-quinolizine-9,5′-4H-isoxazole] 40

Compound **40** was obtained as described in general procedure **B** from chlorooxime **28** as a white solid (184 mg, 49%). mp 92–94 °C. R_f (CH_2Cl_2/MeOH 9/1) 0.21. IR (ATR diamond, cm^{-1}) ν 883, 907, 932, 1031, 1105, 1129, 1228, 1266, 1366, 1439, 1470, 2931. ^{1}H NMR (400 MHz, $CDCl_3$) δ 0.92–1.10 (m, 1H), 1.13–1.37 (m, 1H), 1.41–1.86 (m, 7H), 1.94–2.13 (m, 4H), 2.80–2.95 (m, 2H), 3.00 (d, 1H, J = 17.2 Hz), 3.59 (d, 1H, J = 17.2 Hz), 6.78 (dd, 1H$_{Ar}$, J = 2.2 Hz, J = 1.0 Hz), 7.50 (dt, 1H$_{Ar}$, J = 8.7 Hz, J = 1.0 Hz), 7.65 (d, 1H$_{Ar}$, J = 2.2 Hz), 7.72 (dd, 1H$_{Ar}$, J = 8.7 Hz, J = 1.7 Hz), 7.86 (d, 1H$_{Ar}$, J = 1.7 Hz). ^{13}C NMR (100 MHz, $CDCl_3$) δ 23.2 (CH_2), 24.1 (CH_2), 24.8 (CH_2), 25.9 (CH_2), 37.2 (CH_2), 41.0 (CH_2), 56.6 (CH_2), 56.9 (CH_2), 68.4 (CH), 87.9 (C_q), 107.0 (CH_{Ar}), 112.0 (CH_{Ar}), 120.0 (CH_{Ar}), 123.2 (CH_{Ar}), 125.2 (C_q), 127.9 (C_q), 146.1 (CH_{Ar}), 155.9 (C_q), 156.4 (C_q). HRMS (ESI): *m/z* calculated for $C_{19}H_{23}N_2O_2$ (MH^+): 311.1760; Found: 311.1770.

7.1.24. (9S,9aS)-3′-(5-bromo-2-thienyl)-spiro[8H-quinolizine-9,5′-4H-isoxazole] 41

Compound **41** was obtained as described in general procedure **B** from chlorooxime **29** as a white solid (274 mg, 64%). mp 123–125 °C. R_f (CH_2Cl_2/MeOH 9/1) 0.19. IR (ATR diamond, cm^{-1}) ν 914, 952, 984, 1108, 1126, 1160, 1179, 1230, 1297, 1350, 1445, 2755, 2799, 2852, 2928. ^{1}H NMR (400 MHz, $CDCl_3$) δ 0.87–1.05 (m, 1H), 1.13–1.33 (m, 1H), 1.40–1.83 (m, 7H), 1.88–2.12 (m, 4H), 2.75–2.90 (m, 3H), 3.45 (d, 1H, J = 17.0 Hz), 6.89 (d, 1H, H$_{Ar}$, J = 3.9 Hz), 7.00 (d, 1H, H$_{Ar}$, J = 3.9 Hz). ^{13}C NMR (100 MHz, $CDCl_3$) δ 23.1 (CH_2), 24.0 (CH_2), 24.7 (CH_2), 25.8 (CH_2), 37.0 (CH_2), 40.7 (CH_2), 56.5 (CH_2), 56.8 (CH_2), 68.1 (CH), 88.8 (C_q), 115.7 (C_q), 128.2 (CH_{Ar}), 130.3 (CH_{Ar}), 134.2 (C_q), 151.6 (C_q). HRMS (ESI): *m/z* calculated for $C_{15}H_{20}BrN_2OS$ (MH^+): 355.0480; Found: 355.0475.

7.2. Molecular modeling

Computational results were obtained using software programs from Accelrys Software Inc. The molecules were built and minimized in a molecular package (Discovery Studio® 2.5.5, Accelrys, San Diego, CA) by CHARMm with the CFF partial charge estimation method. The 3D structures were generated and optimized using a CHARMm forcefield with a root mean squared (RMS) difference of energy gradient of 0.1 kcal/mol. The GFA model in the QSAR protocol was used with a population size of 100 and 5000 maximum generations, in linear model form. The descriptors correlation matrix and the results are given in the Supplementary data.

For the 3D-QSAR model, all the structures were superimposed by choosing *N*-1 and *C*-4 (spiranic carbon) on the piperidine scaffold and C-1′ on the first aromatic cycle as tethers to superimpose. The grid spacing was 1.5 Å. For docking studies, the crystal structure of the pentamer AChBP obtained from *Aplysia californica* (Ac-AChBP) with 2-methoxy-4-OH-benzylidene anabaseine (pdb code 2WN9) was used as template [22]. Interaction sites were calculated within a radius of 11.0 Å. The fit was achieved with a maximum rms deviation of 0.7 Å from the interaction sites for each structure, at physiological pH, using the DeNovo protocol.

7.3. Biological studies

Experiments were performed on male Wistar rats weighing 250–300 g (Centre d'Elevage R. Janvier, Le Genest St Isle, France). All animal use procedures were conducted in accordance with the requirements of the European Community Council Directive 2010/63/EU for the care of laboratory animals and with the authorization of the Regional Ethical Committee. Rats were kept in a temperature (23 ± 0.5 °C) and humidity (43 ± 8%) controlled environment under a 12 h light–dark cycle with food and water available *ad libitum*. All efforts were made to minimize animal suffering and discomfort.

Stable α-bungarotoxin and methyllycaconitine were obtained from Tocris Bioscience (R&D Systems, Lille, France) and [^{125}I]α-bungarotoxin (specific activity 81.4 TBq/mmol) from Perkin–Elmer (Courtaboeuf, France).

7.3.1. In vitro binding assays

Animals were killed by decapitation on the day of the assay and both frontal cortices of each animal were removed on ice and weighed (2 rats were used for each experiment). The tissue was homogenized in 10 vol of a pH 7.4 HEPES 15 mM buffer containing 120 mM NaCl, 5.4 mM KCl, 0.8 mM $MgCl_2$ and 1.8 mM $CaCl_2$ using an Ultraturrax T25. After 45,000× g centrifugation at 4 °C for 10 min (J2-21M/E, Beckman), the supernatant was eliminated and the pellet was suspended in 2 mL of the same buffer. The protein concentration was measured according to Bradford using bovine serum albumin as standard.

For competition studies, [^{125}I]α-bungarotoxin (2 nM) was incubated in the presence or absence of each tested compound (10^{-6} to 10^{-10} M) with 25 μg protein in a total volume of 1 mL in a pH 7.4 Tris–HCl buffer (50 mM Tris–HCl, 120 mM NaCl, 5 mM KCl, 1 mM $MgCl_2$ and 2.5 mM $CaCl_2$) for 3 h at 22 °C. Nonspecific binding was determined in the presence of 1 μM α-bungarotoxin. After incubation, samples were diluted in 3 mL of Tris–HCl buffer at 4 °C

and then rapidly filtered through Whatman GF/C fiber filters soaked with 0.05% polyethylenimine (Sigma, St Quentin-Fallavier, France). The filters were washed twice with 3 mL of 4 °C buffer, and the residual radioactivity was measured in a γcounter (2480 Gamma counter Wizard, Perkin Elmer). The IC_{50} values were determined graphically for each compound and the Ki calculated according to Cheng & Prussof [25].

7.3.2. Cerebral biodistribution studies

Rats were injected i.v. under isofurane gas anesthesia in the tail vein with 0.3 mL of **[^{18}F]4** (5 ± 2 MBq) in the control group ($n = 5$). In the MLA group ($n = 5$), injection of the tracer was preceded (15 min) by i.v. injection of methyllycaconitine (3 mg/kg). Rats were killed by decapitation at 1 h post injection of the tracer. The whole brain was quickly removed and dissected into segments consisting of the cortex, striatum, hippocampus, hypothalamus, midbrain and cerebellum. Samples were weighed and radioactivity was measured in the same γ counter as above (counting efficiency of 48% for ^{18}F), and the percent injected dose per gram of tissue (%ID/g) was calculated by comparison with samples to standard dilutions of the injected solution.

7.4. Radiochemistry

7.4.1. N-[(3R)-1-azabicyclo[2.2.2]oct-3-yl]-4-[^{18}F]fluorobenzamide ***[^{18}F]4***

No-carrier-added aqueous ^{18}F-fluoride ion was produced on a cyclotron (PET trace, GE Healthcare) by irradiation of enriched ^{18}O H_2O with protons *via* the $^{18}O(p,n)^{18}F$ nuclear reaction. ^{18}F-Fluoride was transferred to a GE TRACERlab FX-FN synthesizer and passed through an anion-exchange resin (Waters Sep-Pak Accell Light QMA cartridge in the carbonate form). Trapped ^{18}F-fluoride was isolated by elution with a solution of aqueous eluant solution containing K_2CO_3 (7 mg in 300 μL of pure water), acetonitrile (300 μL), and 22 mg of Kryptofix-222 (4,7,13,16,21,24-hexaoxa-1,10-diazabicyclo [8.8.8] hexacosane). Azeotropic drying by addition of ACN (1 mL) was performed. The evaporation was performed at 90 °C under helium flow and vacuum, and the operation was repeated twice. ACN (300 μl) was added to the reactor to solubilize the ^{18}F fluoride which was transferred to the 2 mL reactor of the microwave (PET wave, CEM) containing 2 mg of nitrobenzamide **6** dissolved in DMSO (1 mL). The solution was gently heated to 95 °C for 2 min under helium flow to remove the volatiles. Then, the solution was heated under microwave irradiation at 100 W for 10 min. The solution was cooled and transferred back to the FX-FN synthesizer. The crude product was injected onto a Gemini C18 column (10 × 250 mm, 10 μm) and purification occurred at 5 mL/min using NH_4OAc 0.1M (0.2% Et_3N)/ACN (82:18) as mobile phase. The radioactive peak corresponding to **[^{18}F]4** was collected and diluted with water (30 mL). The radioactive product was trapped on a *t*C18 cartridge (Waters Sep-Pak Accell Light *t*C18 cartridge). The cartridge was rinsed with 5 mL of water and **[^{18}F]4** was eluted from the *t*C18 with EtOH (0.5 mL). Formulation was completed by addition of 0.9% NaCl solution (4.5 mL).

7.5. Cristallography

X-ray analyses were carried out on a Bruker Enraf Nonius CAD4 diffractometer with a Cu sealed tube. The structures were solved by direct methods and refined using the Shelx 97 suite of programs [26] in the integrated WinGX system [27]. The positions of the H atoms were deduced from coordinates of the non-H atoms and confirmed by Fourier synthesis. The non-H atoms were refined with anisotropic temperature parameters. H atoms were included for structure factor calculations but not refined. The program PLATON [28] was used for analysis and drawing figures with thermal ellipsoids at a 30% probability level. Crystallographic data have been deposited in the Cambridge Crystallographic Data Centre (CCDC numbers 952168 and 952169 for compounds **30** and **26** respectively). Copies of these data can be obtained free of charge from the Director CCDC 12 Union Road, Cambridge, CB2 1EZ, UK. Fax: +44 1223 336 033; e-mail: deposit@ccdc.cam.ac.uk or http://www.ccdc.cam.ac.uk/data_request/cif.

Acknowledgments

This research was supported by grants from the Région Centre the ANR Malz program (ANR-10-MALZ-0004) and France Alzheimer. The two teams (ICOA, U930) involved in the project are members of Labex IRON (**ANR-11-LABX-0018-01**). The authors thank Cyclopharma Laboratories for kindly supplying ^{18}F and for use of their laboratory (Laboratoires Cyclopharma, Biopôle Clermont-Limagne, 63360 Saint-Beauzire, France).

Appendix A. Supplementary data

Supplementary data related to this article can be found at http://dx.doi.org/10.1016/j.ejmech.2014.04.057.

References

[1] J. Wu, J.M. Ishikawa, J. Zhang, K. Hashimoto, Brain imaging of nicotinic receptors in Alzheimer's disease, Int. J. Alzheimers Dis. 2010 (2010) 548913;
F. Dajas-Bailador, S. Wonnacott, Nicotinic acetylcholine receptors and the regulation of neuronal signaling, Trends Pharm. Sci. 25 (2004) 317–325.

[2] C. Gotti, M. Zoli, F. Clementi, Brain nicotinic acetylcholine receptors: native subtypes and their relevance, Trends Pharm. Sci. 27 (2006) 482–491;
D. Paterson, A. Nordberg, Neuronal nicotinic receptors in the human brain, Prog. neurobiol. 61 (2000) 75–111.

[3] B. Lendvai, Kassai, Á. Szájli, Z. Némethy, α7 nicotinic acetylcholine receptors and their role in cognition, Brain Res. Bull 93 (2013) 86–96;
R.W. Gould, P.K. Garg, S. Garg, M.A. Nader, Effects of nicotinic acetylcholine receptor agonists on cognition in rhesus monkeys with a chronic cocaine self-administration history, Neuropharmacology 64 (2013) 479–488;
E.D. Edward, D. Levin, B.B. Simon, Nicotinic acetylcholine involvement in cognitive functions in animals, Psychopharmacol 138 (1998) 217–230;
G. Winterer, J. Gallinat, J. Brinkmeyer, F. Musso, J. Kornhuber, N. Thuerauf, D. Rujescu, R. Favis, Y. Sun, M.A. Franc, S. Ouwerkerk-Mahadevan, L. Janssens, M. Timmers, J.R. Streffer, Allosteric alpha-7 nicotinic receptor modulation and P50 sensory gating in schizophrenia: a proof-of-mechanism study, Neuropharmacology 64 (2013) 197–204.

[4] M. Quik, X.A. Perez, T. Bordia, Nicotine as a potential neuroprotective agent for Parkinson's disease, Mov. Disord. 27 (2012) 947–952;
J.R. Tregellas, J. Tanabe, D.C. Rojas, S. Shatti, A. Olincy, L. Johnson, L.F. Martin, F. Soti, W.R. Kem, S. Leonard, R. Freedman, Effects of an alpha 7-nicotinic agonist on default network activity in schizophrenia, Biol. Psychiatry 69 (2011) 7–11;
C. Conejero-Goldberg, P. Davies, L. Ulloa, Alpha7 nicotinic acetylcholine receptor: a link between inflammation and neurodegeneration, Neurosci. Biobehav. Rev. 32 (2008) 693–706;
H.Y. Wang, D.H.S. Lee, M.R. D'Andrea, P.A. Peterson, R.P. Shank, A.B. Reitz, Beta-amyloid(1-42) binds to alpha7 nicotinic acetylcholine receptor with high affinity. Implications for Alzheimer's disease pathology, J. Biol. Chem. 375 (2000) 5626–5632.

[5] E. Zotova, V. Bharambe, M. Cheaveau, W. Morgan, C. Holmes, S. Harris, J.W. Neal, S. Love, J.A.R. Nicoll, D. Boche, Inflammatory components in human Alzheimer's disease and after active amyloid-β42 immunization, Brain 136 (2013) 2677–2696.

[6] N.R. Madadi, N.R. Penthala, L.K. Brents, B.M. Ford, P.L. Prather, P.A. Crooks, Evaluation of (Z)-2-((1-benzyl-1*H*-indol-3-yl)methylene)-quinuclidin-3-one analogues as novel, high affinity ligands for CB1 and CB2 cannabinoid receptors, Bioorg. Med. Chem. Lett. 23 (2013) 2019–2021;
K. Ishida, G. Visbal, J.C. Rodrigues, J.A. Urbina, W. de Souz, S.J. Rozental, Two squalene synthase inhibitors, E5700 and ER-119884, interfere with cellular proliferation and induce ultrastructural and lipid profile alterations in a Candida tropicalis strain resistant to fluconazole, itraconazole, and amphotericin B, Infect. Chemother. 17 (2011) 563–570;
R. Naito, Y. Yonetoku, Y. Okamoto, A. Toyoshima, K. Ikeda, M. Takeuchi, Synthesis and antimuscarinic properties of quinuclidin-3-yl 1,2,3,4-tetrahydroisoquinoline-2-carboxylate derivatives as novel muscarinic receptor antagonists, J. Med. Chem. 48 (2005) 6597–6606;
R.D. Clark, A.B. Miller, J. Berger, D.B. Repke, K.K. Weinhardt, B.A. Kowalczyk,

R.M. Eglen, D.W. Bonhaus, C.H. Lee, A.D. Michel, W.L. Smith, E.H.F. Wong, 2-(Quinuclidin-3-yl)pyrido[4,3-b]indol-1-ones and isoquinolin-1-ones. Potent conformationally restricted 5-HT3 receptor antagonists, J. Med. Chem. 36 (1993) 2645–2657.

[7] R. Tatsumi, K. Seio, M. Fujio, J. Katayama, T. Horikawa, K. Hashimoto, H. Tanaka, (+)-3-[2-(Benzo[*b*]thiophen-2-yl)-2-oxoethyl]-1-azabicyclo[2.2.2]octane as potent agonists for the α7 nicotinic acetylcholine receptor, Bioorg. Med. Chem. Lett. 14 (2004) 3781–3796.

[8] A.L. Bodnar, L.A. Cortes-Burgos, K.K. Cook, D.M. Dinh, V.E. Groppi, M. Hajos, N.R. Higdon, W.E. Hoffmann, R.S. Hurst, J.K. Myers, B.N. Rogers, T.N. Wall, M.L. Wolf, E. Wong, Discovery and structure-activity relationship of quinuclidine benzamides as agonists of alpha7 nicotinic acetylcholine receptors, J. Med. Chem. 48 (2005) 905–908.

[9] D.P. Walker, D.G. Wishka, D.W. Piotrowski, S. Jia, S.C. Reitz, K.M. Yates, J.K. Myers, T.N. Vetman, B.J. Margolis, E.J. Jacobsen, B.A. Acker, V.E. Groppi, M.L. Wolfe, B.A. Thornburgh, P.M. Tinholt, L.A. Cortes-Burgos, R.R. Walters, M.R. Hester, E.P. Seest, L.A. Dolak, F. Han, B.A. Olson, L. Fitzgerald, B.A. Staton, T.J. Raub, M. Hajos, W.E. Hoffmann, K.S. Li, N.R. Higdon, T.M. Wall, R.S. Hurst, E.H. Wong, B.N. Rogers, Design, synthesis, structure–activity relationship, and in vivo activity of azabicyclic aryl amides as α7 nicotinic acetylcholine receptor agonists, Bioorg. Med. Chem. 14 (2006) 8219–8248.

[10] T.A. Hauser, A. Kucinski, K.G. Jordan, G.J. Gatto, S.R. Wersinger, R.A. Hesse, E.K. Stachowiak, M.K. Stachowiak, R.L. Papke, P.M. Lippiell, M. Bencherif, TC-5619: an alpha7 neuronal nicotinic receptor-selective agonist that demonstrates efficacy in animal models of the positive and negative symptoms and cognitive dysfunction of schizophrenia, Biochem. Pharmacol. 78 (2009) 803–812.

[11] A.A. Mazurov, J. Klucik, L. Miao, A.S., Seamans, T. Philips, J.D. Schmitt, C.H. Miller, (2004) WO2004076449.

[12] B.A. Acker, E.J. Jacobsen, B.N. Rogers, D.G. Wishka, S.C. Reitz, D.W. Piotrowski, J.K. Myers, M.L. Wolfe, V.E. Groppi, B.A. Thornburgh, P.M. Tinholt, R.R. Walters, B.A. Olson, L. Fitzgerald, B.A. Staton, T.J. Raub, M. Krause, K.S. Li, W.E. Hoffmann, M. Hajos, R.S. Hurst, D.P. Walker, Discovery of N-[(3R,5R)-1-azabicyclo[3.2.1]oct-3-yl]furo[2,3-*c*]pyridine-5-carboxamide as an agonist of the α7 nicotinic acetylcholine receptor: In vitro and in vivo activity, Bioorg. Med. Chem. Lett. 18 (2008) 3611–3614.

[13] C.J. O'Donnell, B.N. Rogers, B.S. Bronk, D.K. Bryce, J.W. Coe, K.K. Cook, A.J. Duplantier, E. Evrard, M. Hajós, W.E. Hoffmann, R.S. Hurst, N. Maklad, R.J. Mather, S. McLean, F.M. Nedza, B.T. O'Neill, L. Peng, W. Qian, M.M. Rottas, S.B. Sands, A.W. Schmidt, A.V. Shrikhande, D.K. Spracklin, D.F. Wong, A. Zhang, Discovery of 4-(5-methyloxazolo[4,5-*b*]pyridin-2-yl)-1,4-diazabicyclo[3.2.2]nonane (CP-810,123), a novel alpha 7 nicotinic acetylcholine receptor agonist for the treatment of cognitive disorders in schizophrenia: synthesis, SAR development, and in vivo efficacy in cognition models, J. Med. Chem. 53 (2010) 1222–1237.

[14] C. Neagoie, E. Vedrenne, F. Buron, J.Y. Merour, S. Rosca, S. Bourg, O. Lozach, L. Meijer, B. Baldeyrou, A. Lansiaux, S. Routier, Synthesis of chromeno[3,4-b]indoles as Lamellarin D analogues: a novel DYRK1A inhibitor class, Eur. J. Med. Chem. 49 (2012) 379–396;
R. Boulahjar, A. Ouach, M. Chiurato, S. Bourg, M. Ravache, R. Le Guével, S. Marionneau-Lambot, T. Oullier, O. Lozach, L. Meijer, C. Guguen-Guillouzo, S. Lazar, M. Akssira, Y. Troin, G. Guillaumet, S. Routier, Novel tetrahydropyrido[1,2-a]isoindolone derivatives (valmerins): potent cyclin-dependent kinase/glycogen synthase kinase 3 inhibitors with antiproliferative activities and antitumor effects in human tumor xenografts, J. Med. Chem. 55 (2012) 9589–9606;
F. Pin, F. Buron, F. Saab, L. Colliandre, S. Bourg, F. Schoentgen, R. Le Guével, C. Guillouzo, S. Routier, Synthesis and biological evaluation of 2,3-bis(het)aryl-4-azaindole derivatives as protein kinase inhibitors, Med. Chem. Commun. 2 (2011) 899–903;
C. Legros, U. Matthey, T. Grelak, S. Pedragona-Moreau, W. Hassler, S. Yous, E. Thomas, F. Suzenet, B. Folleas, F. Lefoulon, P. Berthelot, D.-H. Caignard, G. Guillaumet, P. Delagrange, J.L. Brayer, O. Nosjean, J.A. Boutin, New radioligands for describing the molecular pharmacology of MT1 and MT2 melatonin receptors, Int. J. Mol. Sci. 14 (2013) 8948–8962.

[15] S. Rötering, M. Scheunemann, S. Fischer, A. Hiller, D. Peters, W. Deuther-Conrad, P. Brust, Radiosynthesis and first evaluation in mice of [18F]NS14490 for molecular imaging of α7 nicotinic acetylcholine receptors, Bioorg. Med. Chem. 21 (2013) 2635–2642;
W. Deuther-Conrad, S. Fischer, A. Hiller, E.Ø. Nielsen, D. Brunicardi-Timmermann, J. Steinbach, O. Sabri, D. Peter, P. Brust, Molecular imaging of alpha7 nicotinic acetylcholine receptors: design and evaluation of the potent radioligand [^{18}F]NS10743, Eur. J. Nucl. Med. Mol. 36 (2009) 791–800;
H.T. Ravert, P. Dorff, C.A. Foss, R.C. Mease, H. Fan, C.R. Holmquist, E. Phillips, D.J. McCarthy, J.R. Heys, D.P. Holt, Y. Wang, C.J. Endres, R.F. Dannal, M.G. Pomper, Radiochemical synthesis and in vivo evaluation of [18F]AZ11637326: An agonist probe for the α7 nicotinic acetylcholine receptor, Nucl. Med. Biol. 40 (2013) 731–739;
Y. Gao, K.J. Kellar, R.P. Yasuda, T. Tran, Y. Xiao, R.F. Dannals, A.G. Horti, Derivatives of dibenzothiophene for positron emission tomography imaging of α7-nicotinic acetylcholine receptors, J. Med. Chem. 56 (2013) 7574–7589.

[16] V. Berdini, M.C. Cesta, R. Curti, G. D'Anniballe, N. Di Bello, G. Nano, L. Nicolini, A. Topai, M. Allegretti, A modified palladium catalysed reductive amination procedure, Tetrahedron 58 (2002) 5669–5674.

[17] A. Tikad, S. Routier, M. Akssira, J.M. Leger, C. Jarry, G. Guillaumet, Efficient access to novel mono- and disubstituted pyrido[3,2-*d*]pyrimidines, Synlett 12 (2006) 1938–1942.

[18] S.T. Tong, D. Barker, A concise synthesis of (±) and a total synthesis of (+)-epiquinamide, Tetrahedron Lett. 47 (2006) 5017–5020.

[19] C. Dallanoce, M. Canovi, C. Matera, T. Mennini, M. De Amici, M. Gobbi, C. De Micheli, A novel spirocyclic tropanyl-Δ2-isoxazoline derivative enhances citalopram and paroxetine binding to serotonin transporters as well as serotonin uptake, Bioorg. Med. Chem. 20 (2012) 6344–6355.

[20] H.J. Böhm, The computer program LUDI: a new method for the de novo design of enzyme inhibitors, J. Comput. Aided Mol. Design. 6 (1992) 61–78.

[21] I. Mueggeand, Y.C. Martin, A general and fast scoring function for protein-ligand interactions: a simplified potential approach, J. Med. Chem. 42 (1999) 791–804.

[22] R.E. Hibbs, G. Sulzenbacher, J. Shi, T.T. Talley, S. Conrod, W.R. Kem, P. Taylor, P. Marchot, Y Bourne, Structural determinants for interaction of partial agonists with acetylcholine binding protein and neuronal alpha7 nicotinic acetylcholine receptor, EMBO J. 28 (2009) 3040–3051.

[23] D.L. Maier, G. Hill, M. Ding, D. Tuke, E. Einstein, D. Gurley, J.C. Gordon, M.J. Bock, J.S. Smith, R. Bialecki, M. Eisman, C. Elmore, J.L. Werkheiser, Preclinical validation of a novel alpha-7 nicotinic receptor radiotracer, [(3)*H*]AZ11637326: target localization, biodistribution and ligand occupancy in the rat brain, Neuropharmacology 61 (2011) 161–171.

[24] S. Routier, F. Suzenet, F. Pin, S. Chalon, J. Vercouillie, D. Guilloteau, (2012) WO2012143526.

[25] Y. Chen, W.H. Prussof, Relationship between the inhibition constant (K1) and the concentration of inhibitor which causes 50 per cent inhibition (I50) of an enzymatic reaction, Biochem. Pharmacol. 22 (1973) 3099–3108.

[26] G.M. Sheldrick, A short history of SHELX, Acta Cryst. A64 (2008) 112–122.

[27] L.J. Farrugia, WinGX suite for small-molecule single-crystal crystallography, J. Appl. Cryst. 32 (1999) 837–838.

[28] A.L. Spek, Single-crystal structure validation with the program PLATON, J. Appl. Cryst. 36 (2003) 7–13.